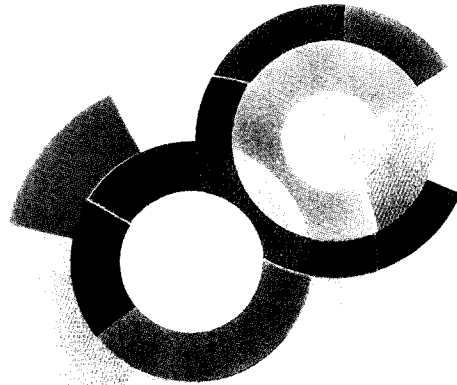
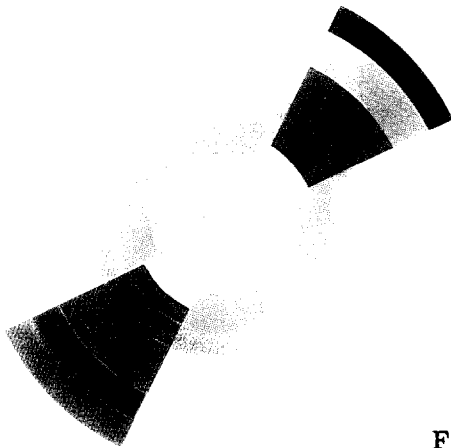
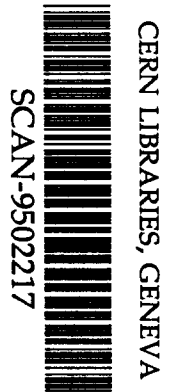


B/B



84 9508



CEA/DAPNIA/SPHn 95 01

01/1995

**First results with the 4π charged particle detector INDRA
at GANIL**

R. Dayras³, G. Auger¹, Ch.O. Bacri², A. Benkirane¹, J. Benlliure¹, B. Berthier³,
B. Borderie², R. Bougault⁴, P. Box², R. Brou⁴, Y. Cassagnou³, J-L. Charvet³,
A. Chbihi¹, J. Colin⁴, D. Cussol⁴, E. De Filippo³, A. Demeyer⁵, D. Durand⁴,
P. Ecomard¹, P. Eudes⁶, A. Genoux-Lubain⁴, D. Gourio⁶, D. Guinet⁵,
L. Lakehal-Ayat², P. Lautesse⁵, P. Lautridou⁶, J.L. Laville⁶, L. Lebreton⁵,
C. Le Brun⁴, J.F. Lecolley⁴, A. Lefevre¹, R. Legrain³, O. Lopez⁴, M. Louvel⁴,
N. Marie¹, V. Métyvier⁴, L. Nalpas³, T. Kakagawa⁴, A. Ouatizerga², M. Parlog²,
J. Péter⁴, E. Plagnol², E.C. Pollacco³, J. Pouthas¹, A. Rahmani⁶, R. Regimbart⁴,
M.F. Rivet², T. Reposeur⁶, E. Rosato⁴, F. Saint-Laurent¹, M. Squali²,
J.C. Steckmeyer⁴, B. Tamain⁴, L. Tassan-Got², E. Vient⁴, C. Volant³,
J.P. Wieleczko¹, A. Wieloch⁴ and K. Yuasa-Nakagawa⁴.

DAPNIA

Le DAPNIA (Département d'Astrophysique, de physique des Particules, de physique Nucléaire et de l'Instrumentation Associée) regroupe les activités du Service d'Astrophysique (SAp), du Département de Physique des Particules Élémentaires (DPhPE) et du Département de Physique Nucléaire (DPhN).

Adresse : DAPNIA, Bâtiment 141
CEA Saclay
F - 91191 Gif-sur-Yvette Cedex

Exposé invité à "Third IN2P3-Riken Symposium
on Heavy Ion Collisions"

Shinrin-Koen, Saitama, Japan

du 24 au 28 Octobre 1994

First results with the 4π charged particle detector INDRA at GANIL

R. Dayras³, G. Auger¹, Ch.O. Bacri², A. Benkirane¹, J. Benlliure¹, B. Berthier³,
B. Borderie², R. Bougault⁴, P. Box², R. Brou⁴, Y. Cassagnou³, J-L. Charvet³,
A. Chbihi¹, J. Colin⁴, D. Cussol⁴, E. De Filippo³, A. Demeyer⁵, D. Durand⁴,
P. Ecomard¹, P. Eudes⁶, A. Genoux-Lubain⁴, D. Gourio⁶, D. Guinet⁵,
L. Lakehal-Ayat², P. Loutesse⁵, P. Lautridou⁶, J.L. Laville⁶, L. Lebreton⁵,
C. Le Brun⁴, J.F. Lecolley⁴, A. Lefevre¹, R. Legrain³, O. Lopez⁴, M. Louvel⁴,
N. Marie¹, V. Métivier⁴, L. Nalpas³, T. Kakagawa⁴, A. Ouatizerga², M. Parlog²,
J. Péter⁴, E. Plagnol², E.C. Pollacco³, J. Pouthas¹, A. Rahmani⁶, R. Regimbart⁴,
M.F. Rivet², T. Reposeur⁶, E. Rosato⁴, F. Saint-Laurent¹, M. Squali²,
J.C. Steckmeyer⁴, B. Tamain⁴, L. Tassan-Got², E. Vient⁴, C. Volant³,
J.P. Wieleczko¹, A. Wieloch⁴ and K. Yuasa-Nakagawa⁴.

(1) GANIL, B.P.5027 - 14021 Caen Cedex, France

(2) IPN, IN2P3-Université Paris Sud, F-91406 Orsay, France

(3) CEA, DAPNIA/SPhN, CE Saclay, F-91191 Gif-sur-Yvette Cedex, France

(4) LPC, ISMRA, IN2P3-CNRS F-14050 Caen Cedex, France

(5) IPN Lyon, IN2P3-CNRS et Université, F-69622 Villeurbanne Cedex, France

(6) SUBATECH, IN2P3-CNRS et Université, F-44072 Nantes Cedex 03, France

Abstract

After a three year construction period, the 4π charged particle detector INDRA took its first data at GANIL, during the spring of 1993. After a brief description of the detector characteristics, an overview of the ongoing scientific program will be given. The general trend of the data will be discussed. For the first time, the energy threshold for the full vaporization of a nuclear system into neutrons and $Z=1$ and 2 isotopes has been determined for the $^{36}\text{Ar}+^{58}\text{Ni}$ reaction. For this system, this threshold is observed for an incident energy of about 50 A.MeV.

I. INTRODUCTION

During the past ten years, great effort has been devoted to determine the maximum energy that a nucleus can sustain before to disintegrate into pieces [1]. These experiments suggest limiting excitation energy decreasing from $\sim 6\text{MeV/u}$ for light

nuclei down to ~ 3 MeV/u for the heaviest nuclei, in fair agreement with theoretical predictions [2] using a soft nuclear equation of state. However, recent data on the system $^{208}\text{Pb}+^{197}\text{Au}$ at 29A.MeV suggest that excitation energies in excess of 6MeV/u can be imparted to nuclei in the mass 200 range [1]. This apparent discrepancy may come in part from the difficulty to define the existence and the excitation energy of a hot nucleus on one hand and the origin of its unstability on the other hand.

Besides emitting neutrons and light charged particles ($Z=1$ and 2), as the excitation energy increases, hot nuclei may decay by emitting intermediate mass fragments (IMF) and eventually break into many fragments (multifragmentation process). Although multi-fragment emission has been observed in many experiments [3], the following questions have not yet received satisfactory answers: *i*)-Is there a continuous evolution from particle evaporation to multifragmentation as the excitation energy increases? *ii*)-Does multifragmentation itself change nature when the limit of stability is reached? *iii*)-What are the respective roles of dynamics and intrinsic properties of the nucleus in the disassembly process? The answer to those questions has been partly hampered by the limitations of the available experimental devices. Indeed, heavy ion collisions at intermediate energies lead to the production of a large number of particles and fragments, the detection of which requires detectors with 4π solid angle coverage, high granularity, low energy detection thresholds and good identification capabilities on an event by event basis. These considerations led us to undertake the construction of INDRA, a high performance charged particle detection array.

In the following, we will give a brief description of the detector, we will then review the scientific program which has been undertaken since 1993 and proceed with a presentation of the first results.

II. THE 4π CHARGED PRODUCT DETECTION ARRAY INDRA

INDRA, a detailed description of which can be found elsewhere [4], can be considered as an ensemble of 336 telescopes covering 90% of the 4π solid angle. The detection cells are distributed amongst 17 rings centered on the beam axis (fig.1). The first ring (2° - 3°) which may sustain a high flux of elastically scattered particles is made of 12 fast counting phoswich scintillators (0.5mm thick NE102 plastic followed by a 25 cm long NE115 plastic). From 3° to 45° , due to the required large energy dynamic range, rings 2 to 9 comprise 132 three-stage telescopes made of an axial field 5cm deep ionization chamber operated at 50mb of C_3F_8 gas, a $300\mu\text{m}$ thick silicon detector and an ICs crystal scintillator thick enough to stop all particles.

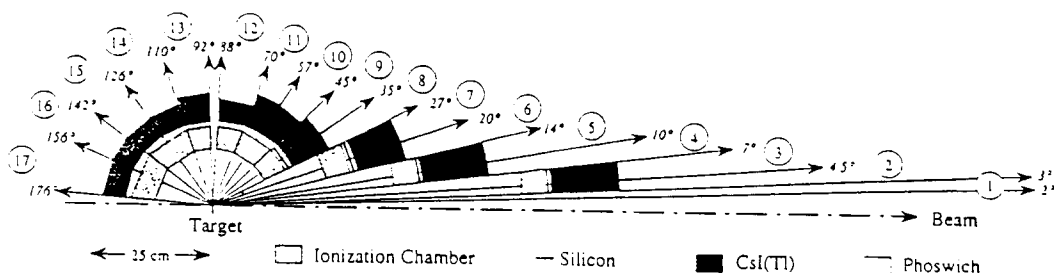


Figure 1. Schematic view of the INDRA detector.

The angular range from 45° to 176° is covered by rings 10 to 17 made of 192 two-stage telescopes each consisting of an axial field ionization chamber operated at 30mb and an ICs crystal scintillator.

All detector signals are treated through specifically designed and highly integrated modules, most of which are in the VXIbus standard. This allows full remote control of the detector parameters, including visualization of signals. Constant monitoring of the detector stability is ensured using a pulsed laser source and electronic pulsers. Great care has been given to the energy calibration of all detection modules, making use of specific detectors and of the secondary beams delivered by the GANIL accelerator.

For fragments with $Z > 3$, charge identification is made through the usual ΔE - E method up to $Z \simeq 50$, down to an energy threshold of $\sim 1A$.MeV. For elements with $Z \leq 3$, isotopic separation is achieved in the ICs crystals using pulse shape discrimination techniques.

III. THE SCIENTIFIC PROGRAM AROUND INDRA

The experimental program around INDRA is mainly oriented towards a better understanding of the properties and of the decay modes of hot nuclei near the limit of stability. Of particular concern is the onset of the multifragmentation process and its dependence upon entrance channel parameters such as bombarding energy, mass asymmetry, total charge and mass of the system.

For very heavy systems, repulsive Coulomb forces may be strong enough to disrupt the total system [2,5] and induce multifragmentation at relatively low bombarding energy ($20 \text{ MeV} < E/A < 40 \text{ MeV}$) where compressional effects are expected to play a

minor role. In order to test this eventuality we have undertaken the study of the systems $^{155}\text{Gd}+^{238}\text{U}$, $^{181}\text{Ta}+^{238}\text{U}$ and $^{238}\text{U}+^{238}\text{U}$.

On the other hand, it has been suggested [6-9] that for light and intermediate mass systems, after an initial compression phase induced by the collision, the nuclear system thus formed expands. During this expansion phase, the system may explore the mechanically unstable spinodal region where it disintegrates into fragments. The connection between this process and a liquid-phase transition for nuclear matter remains an open question. To explore those aspects of nuclear multifragmentation, we have started to investigate the reactions $^{36}\text{Ar}+^{58}\text{Ni}$ and $^{58}\text{Ni}+^{58}\text{Ni}$. Furthermore, with light projectiles such as ^{36}Ar and ^{58}Ni , it is possible, at GANIL, to explore these reactions over a large energy range ($25\text{ MeV} < E/A < 95\text{ MeV}$). This offers the opportunity to study the transverse flow (directed collective motion in the reaction plane of nucleons and clusters emitted in the first stages of the nucleus-nucleus collision), yielding information on the nuclear matter in the interaction zone, such as the modulus of incompressibility or/and the in-medium nucleon-nucleon cross-section [10,11].

The study of symmetric or quasi-symmetric systems such as $^{36}\text{Ar}+\text{KCl}$, $^{58}\text{Ni}+^{58}\text{Ni}$, $^{129}\text{Xe}+^{nat}\text{Sn}$ and $^{181}\text{Ta}+^{197}\text{Au}$ at the same incident energy per nucleon provides the possibility to verify scaling laws [12] in the multifragmentation process whereas other parameters such as the excitation energy per nucleon are kept almost constant.

Finally, the role of the mass asymmetry in the entrance channel can be tested through a comparative study of the two reactions $^{129}\text{Xe}+^{nat}\text{Sn}$ and $^{58}\text{Ni}+^{197}\text{Au}$ which lead to composite systems of almost the same mass.

All these experiments were realized in two campaigns, namely in the spring of 1993 and in the spring of 1994. During each campaign, full energy calibration of all detector modules was performed using α sources, elastically scattered low energy heavy ions as well as secondary light charged particle beams.

In the following, we will give an overview of some results of the first campaign which is not fully analyzed yet.

IV. FIRST RESULTS

In order to minimize energy loss for slow heavy fragments, very thin targets ($< 300\ \mu\text{g}/\text{cm}^2$) were used. Noise in the ionization chambers due to electrons was reduced to an acceptable level by biasing the target to 35 kV [4]. To keep multiple interaction probabilities in the target below 10^{-4} , beam intensities were kept below 10^8 particles/s. Finally, to reject elastic scattering events and the surrounding background,

a low multiplicity ($M \geq 3$ to 5) trigger was used. However, for normalization purpose, few runs were taken with a $M \geq 1$ trigger. With these conditions, the acquisition dead time was around 20%.

As at the time of this talk, energy calibrations are not fully completed yet, only those results using charge identification (and isotopic separation for elements with $Z \leq 3$) and charged product multiplicities will be presented.

A. Charged particle and fragment multiplicities

In fig.2, are presented the total charged product multiplicity distributions as a function of bombarding energy for the two reactions $^{36}\text{Ar} + ^{58}\text{Ni}$ and $^{129}\text{Xe} + ^{\text{nat}}\text{Sn}$. At low bombarding energies, these distributions display a broad bump at high multiplicities which may be imputed to the more central collisions. As the bombarding energy increases, this bump gets shallower whereas the maximum multiplicity increases. For the system $^{36}\text{Ar} + ^{58}\text{Ni}$ at 95 A.MeV, the maximum multiplicity gets close to the total

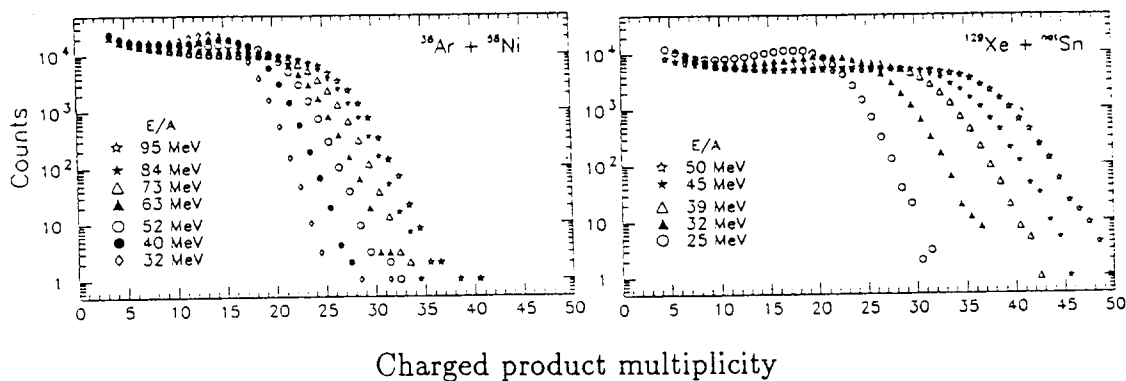


Figure 2. Evolution of the charged product multiplicity distributions with energy for the two systems $^{36}\text{Ar} + ^{58}\text{Ni}$ and $^{129}\text{Xe} + ^{\text{nat}}\text{Sn}$.

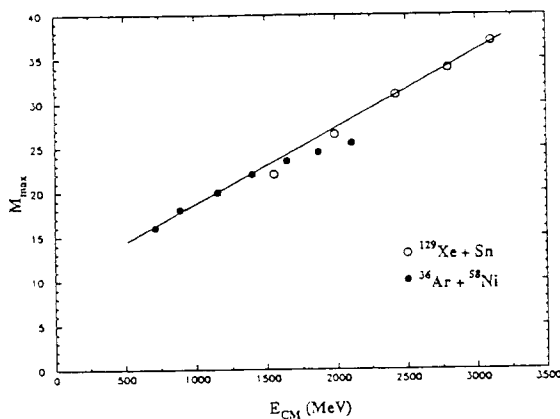


Figure 3. Evolution of the maximum multiplicity with the available c.m. energy for the systems $^{36}\text{Ar} + ^{58}\text{Ni}$ and $^{129}\text{Xe} + ^{\text{nat}}\text{Sn}$.

charge of the system, suggesting a full vaporization of the system into light particles ($Z=1$ and 2).

In fig.3, are reported the maximum multiplicity values taken at the half-maximum of the high multiplicity bump as a function of the available energy in the c.m. frame for the two systems $^{36}\text{Ar}+^{58}\text{Ni}$ and $^{129}\text{Xe}+^{\text{nat}}\text{Sn}$. Independently of the system, the data points lie approximately on a straight line of inverse slope $dE_{cm}/dM \simeq 120$ MeV. In other words, 120 MeV are needed in central collisions to create a new charged particle or fragment. This extremely high value tends to indicate that a large fraction of the available energy is evacuated by non-equilibrium particles before thermalization.

Obviously, the charged product multiplicity is limited by the total charge of the system. Thus as the available energy increases, the maximum charged product multiplicity is expected to saturate as shown by the $^{36}\text{Ar}+^{58}\text{Ni}$ above 1600 MeV available energy. On the other hand for the $^{129}\text{Xe}+^{\text{nat}}\text{Sn}$ which is neutron rich, at low energy, neutron emission is expected to dominate over charged particle emission which will take over at higher energy. This may explain why the maximum charged product

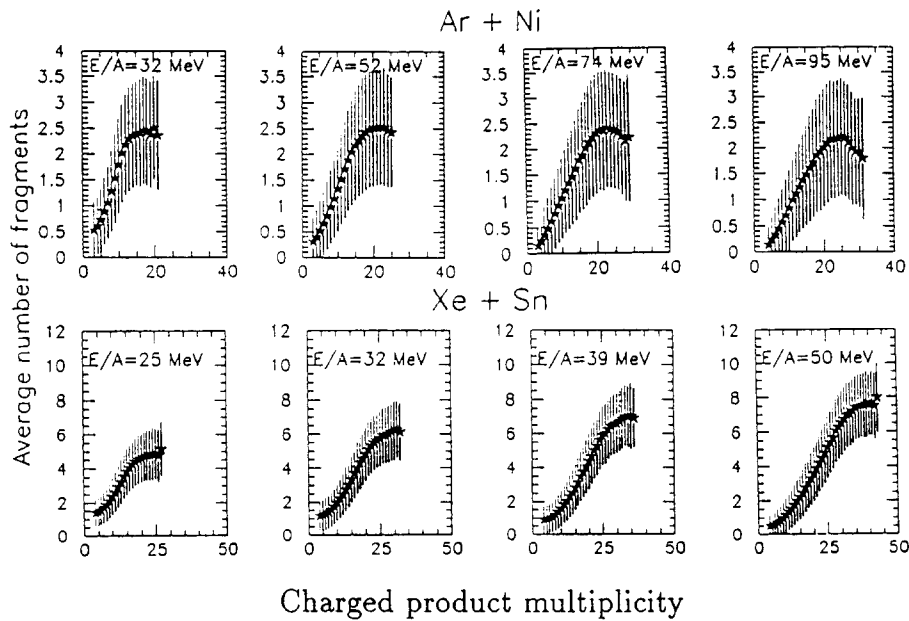


Figure 4. Evolution with bombarding energy of the average number of IMF's ($Z \geq 3$) as a function of the total charged product multiplicity for the two systems $^{36}\text{Ar}+^{58}\text{Ni}$ and $^{129}\text{Xe}+^{\text{nat}}\text{Sn}$. The vertical bars reflect the width of the IMF multiplicity distributions for each value of the total multiplicity.

multiplicity for this system reaches the general trend only above 2 GeV available energy.

Fig.4 gives the evolution of the average number of intermediate mass fragments (IMF) with $Z \geq 3$ as a function of the total charged product multiplicity at different incident energies for the $^{36}\text{Ar}+^{58}\text{Ni}$ and $^{129}\text{Xe}+^{nat}\text{Sn}$ systems. The total charged product multiplicity can be considered as an indication of the violence of the collision or of the impact parameter (the larger is the multiplicity, the more violent is the collision or the smaller is the impact parameter). Starting from low total charged product multiplicity (large impact parameters), the average number of IMF's increases steadily with the total multiplicity to reach a maximum value. Then, depending of the system and of the incident energy, the average number of IMF's either stays constant or it decreases as the total multiplicity continues to increase. For the $^{36}\text{Ar}+^{58}\text{Ni}$ system, the maximum average number of IMF's is ~ 2.5 , independently of the incident energy. Above 50 A.MeV incident energy, the average number of IMF's starts to decrease slowly as the total multiplicity continues to increase. This effect can certainly be imputed to charge conservation. As more and more energy is put into the system, more and more light particles are emitted at the expense of the IMF's. For the much heavier system $^{129}\text{Xe}+^{nat}\text{Sn}$, the maximum average of IMF's increases from ~ 5 at 25 A.MeV to ~ 8 at 50A.MeV. Although the average number of IMF's levels off at high total multiplicity, it never decreases. It has to be noted here that for this system, the available energy per nucleon at 50 A.MeV is about the same that for the $^{36}\text{Ar}+^{58}\text{Ni}$ at 52 A.MeV where the number of IMF's starts to decrease at high total multiplicity. Thus one should expect the same behaviour for the $^{129}\text{Xe}+^{nat}\text{Sn}$ at higher energies.

B. Charge distributions for the $^{36}\text{Ar}+^{58}\text{Ni}$ system.

Few years ago, it has been suggested [13] that, if the disassembly of a nuclear system proceeds through a phase transition of the liquid-gas type [14], the element (or mass) yield distributions at the critical point should follow a power law distribution of the form $\sigma(Z) \propto Z^{-\tau}$, with $\tau \simeq 2.3$. When plotted as a function of the projectile laboratory energy, the τ parameter exhibits a rather universal behaviour [15], irrespective of projectile or target.

In fig.5, are presented the element yield distributions obtained for the system $^{36}\text{Ar}+^{58}\text{Ni}$ as a function of bombarding energy. In order to built these distributions, only well measured events for which the measured charge $Z_{tot} \geq 38$ have been selected. This selection rejects mainly peripheral reactions in which either the projectile-like

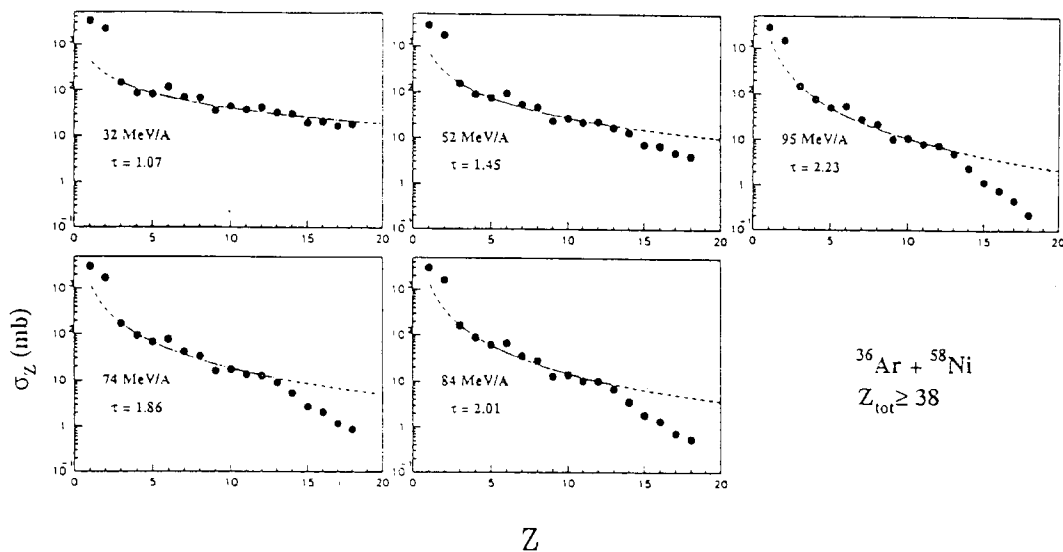


Figure 5. Evolution with bombarding energy of the element yield distributions for well measured events ($Z_{\text{tot}} \geq 38$) in the reaction $^{36}\text{Ar} + ^{58}\text{Ni}$. The curves are power law fits to the data with the indicated values of τ .

fragment escapes detection in the 0° - 2° angular range or/and the target-like fragment is below the energy detection threshold. A power law fit to these distributions could only be obtained over a limited Z -range ($4 \leq Z \leq 13$). The extracted values of the τ parameter increase from 1.07 at 32 A.MeV to 2.23 at 95 A.MeV and are consistent with the systematics from heavy ions induced reactions [15]. However, it has to be noted here, that the Z -distributions plotted as a function of the total charged distributions do not follow a power law but are better fitted by an exponential of the form $\sigma(Z) \propto \exp(-Z/Z_0)$. Thus, the observed power law behaviour of the Z -distributions in the absence of a multiplicity selection, seems to result in the present case from a superimposition of exponential distributions with different values of Z_0 . This casts some doubts on a simple significance of the τ parameter.

C. Vaporization of the $^{36}\text{Ar} + ^{58}\text{Ni}$ system.

By vaporization, it is meant full disintegration of a nuclear system into neutrons, $Z=1$ and $Z=2$ isotopes. Although such a phenomenon is expected when sufficient energy is deposited into the system, its energy threshold has never been established

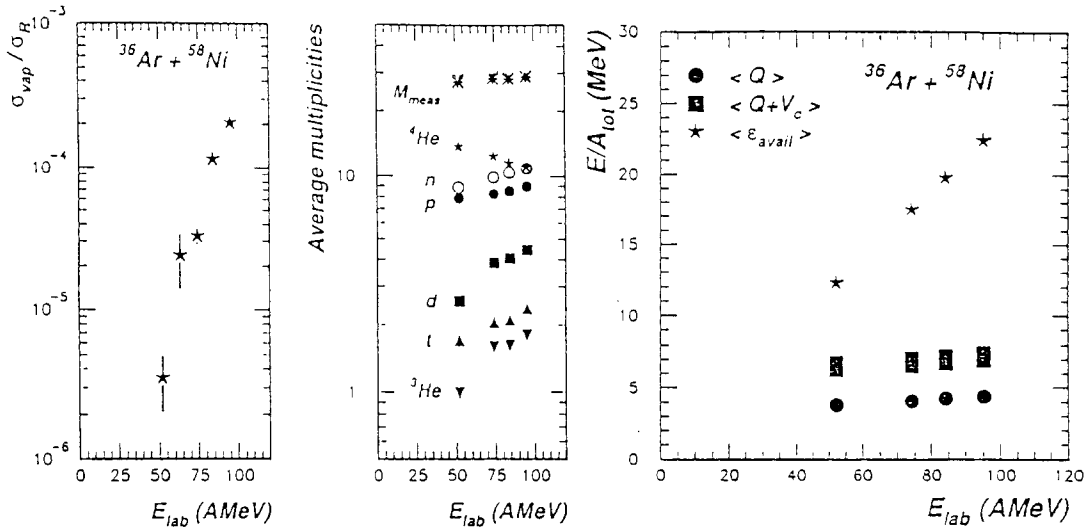


Figure 6. Fraction of vaporization events relative to the reaction cross-section as a function of bombarding energy (left). Evolution of the average light particle multiplicity with incident energy (middle). Mass balance, mass balance+Coulomb energy per nucleon as a function of incident energy (right).

yet. Several theoretical approaches predict such a vaporization process but they differ on its possible link with a liquid-gas phase transition in infinite nuclear matter [16,17].

To select vaporization events, only those events containing solely $Z=1$ and $Z=2$ isotopes and for which the detected charge was greater than 40 (to be compared with 46, the total charge of the system) were retained [18]. Using the measured Z -distributions as a function of the total charge multiplicity, it has been possible to show that for these events, the probability for a fragment with $3 \leq Z \leq 5$ to escape detection was less than 10%. The number of emitted neutrons is readily obtained from mass conservation. The results of this analysis are presented in fig.6. The vaporization cross-section increases by almost two orders of magnitude from 52 A.MeV to 95 A.MeV. The particle production is dominated by alpha particles, the yield of which decreases with bombarding energy whereas the yields of neutrons, protons and deuterons increase. The energetics of the reaction are presented in the right panel of fig.6. The reaction Q -value as well as the Coulomb energy per nucleon are almost independent of bombarding energy. It has to be noted that at 52 A.MeV, the difference between the available energy and the Coulomb+ Q -value energy is $\simeq 6$ MeV per nucleon, close to the limiting excitation energy for intermediate mass nuclei [1].

In the near future, full knowledge of the kinetic energies of all charged particles and fragments should provide a powerful tool to characterize the emission sources and hopefully to better understand the reaction dynamics.

REFERENCES

- [1] D. Guerreau, Nucl. Phys. A574(1994)111c.
- [2] S. Levit and P. Bonche, Nucl. Phys. A437(1985)426.
- [3] L.G. Moretto and G.J. Wozniak, Ann. Rev. Nucl. Part. Sci. 43(1993)379 and references therein.
- [4] J. Pouthas et al. accepted for publication in Nucl. Inst. and Meth.
- [5] B. Borderie, B. Rémaud, M.F. Rivet and F. Sébille, Phys. Rev. Lett. B302(1993)15.
- [6] J. Cugnon, Phys. Lett. B135(1984).374
- [7] J. Aichelin and H. Stöcker, Phys. Lett. B176(1986)14.
- [8] G.F. Bertsch and Ph. Siemens, Phys. Lett. B126(1989)9.
- [9] E. Suraud, D. Cussol, Ch. Grégoire, D. Boiley, M. Pi, P. Schuck, B. Rémaud, and F. Sébille, Nucl. Phys. A495(1989)73c; E. Suraud, M. Pi, P. Schuck, B. Rémaud, F. Sébille, Ch. Grégoire and F. Saint-Laurent, Phys. Lett. B229(1989)359.
- [10] V. de la Mota, F. Sébille, M. Farine, B. Rémaud and P. Schuck, Phys. Rev. C46(1992)677.
- [11] W.Q. Shen et al., Nucl. Phys. A551(1993)333.
- [12] X. Campi, Nucl. Phys. A495(1989)259c; X. Campi and H. Krivine, Nucl. Phys. A545(1992)161c.
- [13] J.E. Finn et al. Phys. Rev. Lett. 49(1982)1321.
- [14] M.E. Fisher Physics 3(1967)225.
- [15] W. Trautmann, U. Milkau, U. Lynen and J. Pochodzalla, Z. Phys. A344(1993)447.
- [16] J.P. Bondorf, R. Donangelo, H. Schulz and K. Sneppen, Phys. Lett. 162B(1985)30.
- [17] D.H.E. Gross, Zhang Xiao-ze and Xu Shu-yan, Phys. Rev. Lett. 56(1986)1544.
- [18] Ch.O. Bacri et al., submitted for publication in Phys. Lett. B.